Published in final edited form as:

NMR Biomed. 2016 September ; 29(9): 1240–1248. doi:10.1002/nbm.3310.

A Simple Approach to Evaluate the Kinetic Rate Constant for ATP Synthesis in Resting Human Skeletal Muscle at 7 T

Jimin Ren[a,b], **A. Dean Sherry**[a,b,c], and **Craig R. Malloy**[a,b,d,e,*]

[a]Advanced Imaging Research Center, University of Texas Southwestern Medical Center, Dallas, TX75390

[b]Department of Radiology, University of Texas Southwestern Medical Center, Dallas, TX75390

[c]Department of Chemistry, University of Texas at Dallas, Richardson, TX75080

[d]Department of Internal Medicine, University of Texas Southwestern Medical Center, Dallas, TX75390

[e]VA North Texas Health Care System, Dallas, TX75216

Abstract

Inversion transfer (IT) is a well-established technique with multiple attractive features for analysis of kinetics. However, its application in measurement of ATP synthesis rate in vivo has lagged behind the more common ST techniques. One well-recognized issue with IT is the complexity of data analysis in comparison to much simpler analysis by ST. This complexity arises, in part, because the γ-ATP spin is involved in multiple chemical reactions and magnetization exchanges, whereas Pi is involved in a single reaction, Pi → γ-ATP. By considering the reactions involving γ-ATP only as a lumped constant, the rate constant for the reaction of physiological interest, $k_{Pi\rightarrow\gamma ATP}$, can be determined. Here, we present a new IT data analysis method to evaluate $k_{Pi\rightarrow\gamma ATP}$ using data collected from resting human skeletal muscle at 7T. The method is based on the basic Bloch-McConnell equation, which relates $k_{Pi\rightarrow\gamma ATP}$ with $\dot{m}_{Pi}$, the rate of Pi magnetization change. The $k_{Pi\rightarrow\gamma ATP}$ value is accessed from $\dot{m}_{Pi}$ data by more familiar linear correlation approaches. For a group of human subjects (n = 15), the $k_{Pi\rightarrow\gamma ATP}$ value derived for resting calf muscle was 0.066 ± 0.017 s^{-1}, in agreement with literature reported values. In this study we also explored possible time-saving strategies to speed up data acquisition for $k_{Pi\rightarrow\gamma ATP}$ evaluation using simulations. The analysis indicates that it is feasible to carry out a ^{31}P inversion transfer experiment in ~10 minutes or shorter at 7T with reasonable outcome in $k_{Pi\rightarrow\gamma ATP}$ variance for measurement of ATP synthesis in resting human skeletal muscle. We believe that this new IT data analysis approach will facilitate the wide acceptance of IT to evaluate ATP synthesis rate in vivo.

Keywords

skeletal muscle; magnetization transfer; ATP; chemical exchange; T1 relaxation time; 7T; inversion transfer; energy metabolism

*To whom correspondence should be addressed. Craig R. Malloy, 5323 Harry Hines Blvd, NE4.2, Dallas, Texas 75390-8568, USA, (214) 645-2722, craig.malloy@utsouthwestern.edu.

INTRODUCTION

Saturation transfer (ST) and inversion transfer (IT) are two techniques to probe the kinetics of magnetization exchange (ME) between spins at different resonance frequency (1–6). ^{31}P NMR and ST have been the preferred techniques for noninvasive analysis of high energy phosphate metabolism for the last three decades (7–20). Extension of ST to high magnetic fields should be advantageous because of improved sensitivity, but implementation of prolonged saturating pulses in human subjects may be challenging because of hardware and SAR limitations, and additional data must be acquired to correct for off-resonance saturation, the so-called "spillover" effect (21,22), in spite of increased chemical shift dispersion (23). Inversion transfer may be technically simpler to implement at high fields, and it offers the advantages of low SAR, an inherently large initial labeling effect (Mz → -Mz *versus* Mz → 0), and insensitivity to “spillover” side effect.

Despite these potential advantages and applications in a number of kinetic studies (3–6,24–27), the inversion transfer technique is rarely used to measure the rate constant ($k_{Pi\rightarrow ATP}$) for ATP synthesis in vivo while ST has been the method of choice (7–20,28–34). One reason that ST is so popular is that the prolonged saturation (5 – 9 seconds) at γ-ATP allows magnetization transfer effects to build up in Pi despite the intrinsically slow Pi ↔ γ-ATP exchange rate. Frequency-selective inversion at γ-ATP is limited by the relatively fast relaxation of the γ-ATP spin (apparent T_1 relaxation ~ 1 – 2 sec) and consequently the duration of any magnetization transfer effect is brief. At higher magnetic fields, the increased effect of chemical shift anisotropy further accelerates T_1 relaxation of ATP ^{31}P spins. Our recent work has shown that the problem of fast relaxing γ-ATP can be overcome by using a band-selective inversion of multiple ^{31}P resonances at 7T (35). Co-inversion of phosphocreatine (PCr) and all exchanging ATP spins results in a longer apparent T_1 relaxation of γ-ATP because the inverted magnetization is stored in the longer T_1 PCr pool (~ 5 – 6 sec). This approach leads to an increase in the magnetization transfer effect at Pi, making it suitable for quantitative evaluation of $k_{Pi\rightarrow ATP}$ at 7T.

Analysis of inversion transfer data, however, is complex. The high-energy phosphate exchanges in vivo are described by a five-spin network including ^{31}P in Pi, PCr, α-, β- and γ-ATP. In addition to the well-known chemical exchanges, intramolecular NOE effects have also been identified between γ-ATP ↔ β-ATP and between γ-ATP ↔ α-ATP (6,34,36). For such a complex system a full analytical solution is difficult to achieve. Instead, a numerical solution, although not intuitive, is more practical (6). In contrast to analysis of IT data, the complexity of the ^{31}P spin exchange system in vivo does not affect ST data analysis because upon saturation of γ-ATP, the magnetization of Pi is uncoupled from the rest of the exchange network, resulting in a simple analytical solution to relate the Pi signal reduction and T_1 relaxation time to $k_{Pi\rightarrow ATP}$ (7,10,23).

In this study, we outline a new IT data analysis approach to obtain $k_{Pi\rightarrow ATP}$ based on a single Bloch-McConnell differential equation defined for Pi. By direct access to the rate of Pi magnetization change, it eliminates the need to solve the Bloch-McConnell differential equations for other exchange spins (PCr, α-, β- and γ-ATP) (Figure 1), thereby permitting

an evaluation of $k_{Pi\rightarrow ATP}$ graphically by simple linear regression. The validity of this data analysis approach is demonstrated using datasets acquired from resting human calf muscle using EBIT, a band-selective inversion technique (35). We believe that this new IT data analysis approach will facilitate the wide acceptance of IT to evaluate ATP synthesis rate in vivo, a rate of fundamental importance in physiology (9–20).

METHODS

Theory

For the chemical exchange reaction $Pi \leftrightarrow \gamma - ATP$, after applying an inversion pulse at $\gamma - ATP$ either frequency-selective or band-selective, the rate of change in Pi Z-magnetization M_z (for clarity, the subscript "z" is omitted hereafter) in the inversion delay time t, can be described by the Bloch-McConnell equation as follows,

$$\dot{M}_{Pi}=\frac{M^o_{Pi}-M_{Pi}}{T_{1,Pi}}-k_{Pi\rightarrow\gamma ATP}M_{Pi}+k_{\gamma ATP\rightarrow Pi}M_{\gamma\mathrm{ATP}} \quad [1]$$

where k denotes pseudo first-order kinetic rate constant, with the forward and reverse rate constants related by

$$k_{\gamma ATP\rightarrow Pi}=k_{Pi\rightarrow\gamma ATP}\frac{M^o_{Pi}}{M^o_{\gamma ATP}} \quad [2]$$

in which M^o_{Pi} and $M^o_{\gamma ATP}$ denote the Z-magnetization at Boltzmann thermal equilibrium for Pi and γ-ATP, respectively. Substituting $k_{\gamma ATP\rightarrow Pi}$ in Eq [1] by Eq [2] gives:

$$\dot{m}_{Pi}=\frac{1-m_{Pi}}{T_{1,Pi}}-k_{Pi\rightarrow\gamma ATP}(m_{Pi}+m_{\gamma ATP}) \quad [3]$$

This expression can be rearranged into two different linear equations:

$$\frac{\dot{m}_{Pi}}{1-m_{Pi}}=\frac{1}{T_{1,Pi}}-k_{Pi\rightarrow\gamma ATP}\frac{m_{Pi}-m_{\gamma ATP}}{1-m_{Pi}} \quad [3a]$$

and

$$\frac{\dot{m}_{P_i}}{m_{P_i}-m_{\gamma ATP}}=\frac{1-m_{Pi}}{m_{Pi}-m_{\gamma ATP}}\frac{1}{T_{1,Pi}}-k_{Pi\rightarrow\gamma ATP} \quad [3b]$$

where m is the normalized Z-magnetization defined by:

$$m=M_i/M_i^o \quad (i=\mathrm{Pi},\gamma-\mathrm{ATP}) \quad [4]$$

Eq [3] indicates that two separate terms contribute to $\dot{m}_{Pi}$: the first is the T_1 relaxation term, expressed as the product of $1/T_{1,Pi}$ by $(1 - m_{Pi})$, and the second is the chemical exchange term, expressed as the product of $k_{Pi\rightarrow\gamma ATP}$ by $(m_{Pi} - m_{\gamma ATP})$. Note that the quantity $(1 - m_{Pi})$ represents the exchange effect observed at Pi and that the quantity $(m_{Pi} - m_{\gamma ATP})$ represents the net difference in normalized magnetization between Pi and γ-ATP. Since both $(1 - m_{Pi})$ and $(m_{Pi} - m_{\gamma ATP})$ are experimentally measurable, those two unknowns $T_{1,Pi}$ and $k_{Pi\rightarrow\gamma ATP}$ in Eq [3] thus can be solved by a simple linear fitting to $\dot{m}_{Pi}$. Alternatively, the parameters $k_{Pi\rightarrow\gamma ATP}$ and $1/T_{1,Pi}$ can be evaluated graphically from the intercept or slope of the linear relationship $\frac{\dot{m}_{Pi}}{1-m_{Pi}}$ *versus* $\frac{m_{Pi}-m_{\gamma ATP}}{1-m_{Pi}}$, or $\frac{\dot{m}_{P_i}}{m_{P_i}-m_{\gamma ATP}}$ *versus* $\frac{1-m_{Pi}}{m_{Pi}-m_{\gamma ATP}}$, as defined by Equations [3a] and [3b].

It is clear from Eqs [3, 3a and 3b] that, in order to obtain $k_{Pi\rightarrow\gamma ATP}$ and $1/T_{1,Pi}$, the value of $\dot{m}_{Pi}$ must be known. A way to obtain $\dot{m}_{Pi}$ is first to construct the mathematical equation for the function $m_{Pi}(t)$, from which $\dot{m}_{Pi}(t)$ values can be obtained. With the boundary conditions $m_{Pi}|_{t=0} = 1$ and $m_{Pi}|_{t\rightarrow\infty} = 1$, the time-dependent function of m_{Pi} can be described by

$$m_{Pi}=1-a(e^{-\lambda_1 t}-e^{-\lambda_2 t}) \quad [5]$$

where a, λ_1 and λ_2 are three constants, which can be accessed by numerical fitting the $m_{Pi} \sim t$ dataset. With these three constants, it is straightforward to derive the $\dot{m}_{Pi}$ values using the following differential equation (by applying $\partial/\partial t$ operation on Eq [5]),

$$\dot{m}_{Pi}=a(\lambda_1 e^{-\lambda_1 t}-\lambda_2 e^{-\lambda_2 t}) \quad [6]$$

Based on Eq [3], one may also estimate the parameters $k_{Pi\rightarrow\gamma ATP}$ and $T_{1,Pi}$ from the experimental $m_{Pi} \sim t$ curve at a few special time points.

One example occurs when $\dot{m}_{Pi}(t)=0$ the transition point at which the curve $m_{Pi} \sim t$ reaches a minimum and the effect of chemical exchange reaches the maximum.

$$0=\frac{1-m_{Pi}}{T_{1,Pi}}-k_{Pi\rightarrow\gamma ATP}(m_{Pi}-m_{\gamma ATP})$$

or

$$k_{Pi\rightarrow\gamma ATP}=\frac{1-m_{Pi}}{m_{Pi}-m_{\gamma ATP}}\frac{1}{T_{1,Pi}} \quad (t=t^{\min}) \quad [7]$$

This particular time point is denoted by t^{min}. Equation [7] is equivalent to the formula given by Kuchel (1).

A second example is at $t = 0$, immediately after the inversion of γ-ATP, at which $m_{Pi} = 1$ but $\dot{m}_{Pi} \neq 0$. At this initial time point, the T_1 relaxation term in Eq [3] becomes zero, and $\dot{m}_{Pi}$ is given by:

$$\dot{m}_{Pi}=k_{Pi\rightarrow\gamma ATP}(1-m_{\gamma ATP}(0)) \quad (t=0) \qquad [8]$$

Equation [8] is equivalent to the formula given by Malloy et al (5).

For description of γ-ATP signal, the Bloch-McConnell-Solomon formula has to be used which contains more exchange terms contributed from five pools (Figure 1):

$$\dot{M}_{\gamma ATP}=\frac{M^o_{\gamma ATP}-M_{\gamma ATP}}{T_{1,\gamma ATP}}-k_{\gamma ATP\rightarrow Pi}M_{\gamma ATP}+k_{Pi\rightarrow\gamma ATP}M_{\mathrm{Pi}}-k_{\gamma ATP\rightarrow PCr}M_{\gamma ATP}+k_{PCr\rightarrow\gamma ATP}M_{\mathrm{PCr}}+\sigma(M^o_{\beta ATP}-M_{\beta ATP})-\rho_{\gamma ATP\rightarrow\beta ATP}M_{\gamma ATP}+\rho_{\beta ATP\rightarrow\gamma ATP}M_{\beta ATP} \qquad [9]$$

where σ denotes the rate constant for the cross-relaxation between γ-ATP and β-ATP (NOE) and ρ denotes the rate constant for the chemical exchange between γ-ATP and β-ATP mediated by AK. If all chemical exchange and cross-relaxation effects among PCr, γ-, β-, and α-ATP are lumped in one single pool represented by γ-ATP, then a two-pool model will apply. Under the condition of band inversion with co-inversion of PCr and all ATP spins, this simplified two-pool exchange model yields:

$$\dot{M}_{\gamma ATP}=\frac{M^o_{\gamma ATP}-M_{\gamma ATP}}{T_{1\mathrm{app},\gamma ATP}}-k_{\gamma ATP\rightarrow Pi}M_{\gamma ATP}+k_{Pi\rightarrow\gamma ATP}M_{\mathrm{Pi}} \qquad [10]$$

where $T_{1app,\gamma ATP}$ denotes the apparent T_1 relaxation time of γ-ATP, which lumps T_1 relaxation and all exchange effects together except the exchange pathway involving Pi (Figure 1). In other words, the interaction of γ-ATP with other ^{31}P spins in PCr, ADP and ATP is treated as part of molecular "lattice" and is incorporated into $T_{1app,\gamma ATP}$ (35). Using this approximation, the $k_{Pi\rightarrow\gamma ATP}$ and $T_{1,Pi}$ values can be evaluated numerically by the following matrix equation:

$$M(t)=M^o-e^{At}(M^o-M(0)) \qquad [11]$$

in which $M^o=[M^o_{Pi};M^o_{\gamma ATP}]$; $M(0) = [M_{Pi}(0); M_{\gamma ATP}(0)]$, which is the initial Z-magnetization immediately after band inversion; and A is the exchange matrix

$$A=\begin{bmatrix} -1/T_{1,Pi}-k_{Pi\to\gamma ATP} & k_{\gamma ATP\to Pi} \\ k_{Pi\to\gamma ATP} & -1/T_{1\mathrm{app},\gamma ATP}-k_{\gamma ATP\to Pi} \end{bmatrix} \quad [12]$$

Note that, unlike Eqs [3,3a,3b], Equation [11] contains an additional unknown parameter $T_{1app,\gamma ATP}$ through the matrix A.

Human Subjects

The protocol was approved by the Institutional Review Board of the University of Texas Southwestern Medical Center. Prior to the MRS study, informed written consent was obtained from all participants. Fifteen subjects (9 male and 6 female), aged 27 ± 4 yr and BMI 24 ± 2, participated in the study. Spectra from 10 subjects reported elsewhere (35) were reanalyzed using the new methods, and new data from 5 subjects were acquired and analyzed. All subjects were in good general health with no history of peripheral vascular, systemic or myopathic diseases. To avoid possible exercise-associated physiological variations among subjects, all subjects were asked to refrain from any physical activity of moderate or high intensity for 24 hours prior to the study, and subjects sat at rest for 20 minutes prior to the scan. Heart rate and blood oxygen saturation level were monitored during the scan. The study was well-tolerated by all subjects.

MRS Protocol

The general MRS acquisition protocol has been described previously (35). Briefly, FID-based ^{31}P spectra were acquired from calf muscle for each subject using a band-selective inversion sequence (180° – t – 90° – τ), which was comprised of an adiabatic inversion pulse, followed by a varying inversion delay time t, a hard 90° readout pulse, and a recovery period τ. The inversion time was varied from 30 to 10000 ms with 12 data points spaced logarithmically (t = 30, 626, 1253, 1923, 2641, 3414, 4252, 5167, 6174, 7294, 8556 and 10000 msec). The inversion pulse is a trapezoid-shaped adiabatic pulse with 42 ms duration and an excitation frequency band of 2500 Hz, centered at 150 Hz upfield from α-ATP, which is set to co-invert PCr and ATP spins but not Pi and PDE. Other NMR parameters were TR 30 sec, NA 4 averages, 4 K sampling points zero-filled to 8 K. The chemical shift of the ^{31}P MR spectra was referenced to PCr at 0 ppm. Each ^{31}P NMR spectrum was Fourier transformed, processed with Gaussian apodization (6 Hz) using the scanner software (SpectroView, Philips Healthcare), and further analyzed using Matlab (Mathworks) routines to evaluate the normalized magnetization for Pi, PCr, α-, β- and γ-ATP, based on the magnitude of the observed ^{31}P peaks. The m_{Pi} data were fitted by Equation [5] to obtain the fitting parameters a, λ_1 and λ_2.

To evaluate the exchange rate constant $k_{Pi\to\gamma\text{-}ATP}$ and T_1 value for Pi, the $\dot{m}_{Pi}$ values were first obtained by Eq [6]. Then these $\dot{m}_{Pi}$ data were fit by Eq [3] against the quantities (1 − m_{Pi}) and (m_{Pi} − $m_{\gamma ATP}$). Alternatively, simpler linear relationship can be obtained to evaluate $k_{Pi\to\gamma\text{-}ATP}$ and $T_{1,Pi}$ by plotting $\frac{\dot{m}_{Pi}}{1-m_{Pi}}$ *versus* $\frac{m_{Pi}-m_{\gamma ATP}}{1-m_{Pi}}$, or $\frac{\dot{m}_{P_i}}{m_{P_i}-m_{\gamma ATP}}$

versus $\frac{1-m_{Pi}}{m_{Pi}-m_{\gamma ATP}}$, as defined by Eqs [3a and 3b] respectively. Note that, since the quantity $(1 - m_{Pi})$ appears as denominator in Eq [3a], we chose to exclude the first data point with $(1 - m_{Pi}) \sim 0$ from data analysis. For comparison, the $k_{Pi\rightarrow\gamma\text{-}ATP}$ and $T_{1,Pi}$ values were also obtained by solving Eq [11] numerically.

To examine the reliability of these different evaluation approaches, the $k_{Pi\rightarrow\gamma\text{-}ATP}$ and T_1 values for Pi were also analyzed from the simulated m_{Pi} and $m_{\gamma ATP}$ datasets generated using a set of known parameters ($T_{1,P}$ = 6.5 sec, $T_{1app,\gamma ATP}$ = 4.0 sec, $k_{Pi\rightarrow\gamma\text{-}ATP}$ = 0.065 sec^{-1}, and $M^o_{\gamma\text{-}ATP} / M^o_{Pi}$ = 2.6) at varying delay time (30 – 10000 msec, 12 data points) based on 2-site chemical exchange model. To imitate the effect of spectral background noise on small Pi signal, the m_{Pi} dataset was modulated by pseudo-random noise with a Gaussian distribution variance of 2% (σ ranged from −1% to 1%) generated by Box Muller transformation. A total of 1000 noise-mixed m_{Pi} datasets were analyzed using a self-written Matlab routine for evaluation of the variance in $k_{Pi\rightarrow\gamma\text{-}ATP}$ and $T_{1,Pi}$ values.

An interesting feature embedded in Eqs [3, 3a and 3b] is the absence of $T_{1app,\gamma ATP}$ in $\dot{m}_{Pi}$. To test this feature, simulated m_{Pi} and $m_{\gamma ATP}$ datasets were generated at varying $T_{1app,\gamma ATP}$ values (1, 2, 4, and 6 sec) to examine its effect on the outcome of $k_{Pi\rightarrow\gamma\text{-}ATP}$ and $T_{1,pi}$.

Our in vivo ^{31}P study takes a total scan time of 24 minutes for collecting a series of 12 spectra at varying inversion delay times with constant TR of 30 s and 4 repeated acquisitions. Determination of $k_{Pi\rightarrow\gamma\text{-}ATP}$ and $T_{1,Pi}$ as rapidly as possible is an important experimental goal, and for this reason, the following scenarios were examined by simulations. In simulation #1 (denoted as S1), the noise level was doubled (σ ranged from −2% to 2% in Gaussian distribution), corresponding to one single data acquisition for each inversion time data point, or a simulated total scan time of 6 minutes for the whole series with 12 delay times. In simulation #2 (denoted as S2), only the first 6 data points in the inversion delay series were sampled (inversion delay time = 30, 626, 1253, 1923, 2641, and 3414 msec), corresponding to a scan time of 12 minutes. In simulation #3 (denoted as S3), 6 data points were acquired at large intervals (inversion delay time = 30, 1253, 2641, 4252, 6174, and 8556 msec), which also corresponds to a reduced scan time of 12 minutes.

Statistical Analysis

All data are reported as mean ± standard deviation, calculated using standard functions in Matlab.

RESULTS

Observation of magnetization exchange between Pi and γ-ATP

As illustrated in Figure 2, the increased chemical shift dispersion at ultra-high field 7T facilitates band-selective inversion. Upon co-inversion of ATP and PCr signals, the intensity of Pi signal in calf muscle is significantly reduced due to Pi ↔ γ-ATP exchange as shown (Figure 2e, n = 15 subjects). In contrast, there is no change in signal intensity of PDE (Figure 2e), a relatively inert metabolite not actively involved in exchange with other high energy phosphates in vivo. The absence of effect of the inversion pulse on the PDE signal

illustrates the limited spillover to the Pi signal. As anticipated, the Pi signal continues to decrease as the inversion delay time t increases. After reaching a minimum in intensity, the Pi signal gradually recovers back to the equilibrium state with a further increase in t (Figure 2e). Such a biphasic feature of Pi signal change was clearly observed in the ^{31}P spectra of all subjects studied (n = 15); the maximal reduction of Pi signal ranged from 13 to 21 % and typically occurred between t ~ 3.4 – 4.5 sec (Figure 3).

Unlike the non-inverted ^{31}P signals (Pi and PDE), all the inverted signals (PCr, α-, β- and γ-ATP) recovered exponentially with t (Figure 3 and Supplementary Figure 1S), but at varying recovery rates (PCr < γ-ATP < β-ATP < α-ATP). Notably, the recovery of γ-ATP becomes much slower than that of α- and β-ATP, and more similar to the trend observed for PCr. This yields a long period of delay time with ($m_{Pi} - m_{\gamma ATP}$) > 0, the driving factor for producing the ME effect at Pi (Figure 3a). As will be clear later, to be able to contribute to the net buildup of the ME effect at Pi, the exchange term $k_{Pi\rightarrow\gamma ATP}(m_{Pi} - m_{\gamma ATP})$ has to be sufficiently large to overcome the draining effect of the T_1 relaxation term $(1 - m_{Pi})/T_{1,Pi}$, which occurs only in the period t = 0 ~ 4 sec during which the ME effect $(1 - m_{Pi})$ is in a trend of increase (Figure 3a).

Evaluation of $\dot{m}_{Pi}$ from m_{Pi}

To take advantage of the simple relationship between $\dot{m}_{Pi}$ and $k_{Pi\rightarrow\gamma\text{-}ATP}$, as described by Bloch-McConell equation [3] or its two simpler linear forms (Eqs [3a] and [3b]), for calculation of $k_{Pi\rightarrow\gamma\text{-}ATP}$, the first step is to evaluate the $\dot{m}_{Pi}$ values. These values were derived by Eq [6] using the fitting constants (a, $\lambda 1$ and $\lambda 2$) obtained by fitting the experimental $m_{Pi}(t)$ data (Figure 3a) according to Eq [5]. As shown in Figure 3b (n = 15 subjects), with increase in inversion delay time, the $\dot{m}_{Pi}$ values is changed from negative to positive, with transition occurring at t^{min} ~ 4 sec. Within t = 0 – 4 sec, the $\dot{m}_{Pi}$ magnitude decreases with t (Figure 3b). However, a further increase in inversion delay time (t > 4 sec) leads to a rise and then fall in the $\dot{m}_{Pi}$ magnitude, with a maximum occurring at t ~ 7.3 (Figure 3b). This feature is not visually identifiable in the curve m_{Pi} ~ t (Figure 3a), but becomes obvious when the $\dot{m}_{Pi}$ value is separated into the relaxation and exchange term by Eq [3] (Figure 4b).

Evaluation of $k_{Pi\rightarrow\gamma\text{-}ATP}$ from $\dot{m}_{Pi}$

The simplest way to assess $k_{Pi\rightarrow\gamma\text{-}ATP}$ is to divide $\dot{m}_{Pi}$ value by ($m_{Pi} - m_{\gamma ATP}$) at t = 0 (Eq [8]). This yielded 0.076 ± 0.014 s^{-1} using the measurements at the first data point (t = 0.03 sec) as an approximation. The value of $k_{Pi\rightarrow\gamma\text{-}ATP}$ can also be estimated, if $T_{1,Pi}$ is known, from the ratio $(1 - m_{Pi}) / (m_{Pi} - m_{\gamma ATP})$ at $\dot{m}_{Pi}$ = 0 when $t = t^{min}$ (Eq. [7]). This yielded a $k_{Pi\rightarrow\gamma\text{-}ATP}$ value in the range 0.048 – 0.096 s^{-1} assuming a possible $T_{1,Pi}$ ranging from 3.5 sec (37) to 7.0 sec (6).

To evaluate $k_{Pi\rightarrow\gamma\text{-}ATP}$ by linear graphic approach, we plotted the data $\frac{\dot{m}_{Pi}}{1 - m_{Pi}}$ *against* $\frac{m_{Pi} - m_{\gamma ATP}}{1 - m_{Pi}}$, (Figure 3c) and $\frac{\dot{m}_{Pi}}{m_{Pi} - m_{\gamma ATP}}$ *against* $\frac{1 - m_{Pi}}{m_{Pi} - m_{\gamma ATP}}$ (Figure 3d), using the above-derived $\dot{m}_{Pi}$ values (n = 15 subjects). Both datasets yielded a remarkably good linear

relationship ($y = -0.069\ x + 0.181$ and $R^2 = 0.996$ in Figure 3c, and $y = 0.159\ x - 0.061$ and $R^2 = 0.997$), as anticipated from Eqs [3a] and [3b], respectively. More importantly, the resultant $k_{Pi\rightarrow\gamma\text{-}ATP}$ values from two different linear datasets agreed reasonably well, as summarized in Table 1. In addition, a direct $\dot{m}_{Pi}$ fitting by Eq [3] also yielded an excellent linear correlation ($y = 0.996x + 0.002$ and $R^2 = 0.996$, Figure 4a), with $k_{Pi\rightarrow\gamma\text{-}ATP}$ result (Table 1) comparable to those by other two linear methods (Eqs [3a] and [3b]) and by the numeric matrix approach (Eq [11]). On average, these three different linear data analysis methods yielded a rate constant $k_{Pi\rightarrow\gamma\text{-}ATP}$ of 0.066 ± 0.017 sec^{-1} and $T_{1,Pi}$ value of 5.75 ± 1.91 sec for the group of the subjects studied (n = 15). An apparent T_1 value of 4.02 sec was also obtained by the numeric matrix approach for γ-ATP. Additionally, the fitting procedure by Eq [3] also provides a quantitative separation of $\dot{m}_{Pi}$ into two parts distributable to relaxation- and exchange-related terms, respectively, which clearly illustrates the evolution of these two terms over the inversion delay time (Figure 4b).

The Pi → ATP flux in resting skeletal muscle was 8.47 ± 2.18 mmol/kg wet weight, calculated by the product of the above-derived $k_{Pi\rightarrow\gamma\text{-}ATP}$ value, and the Pi concentration of 2.14 mmol/kg wet weight measured from the integral of Pi signal at 4.83 ppm in reference to that of γ-ATP (5.5 mmol/kg wet weight) in fully relaxed ^{31}P MR spectrum.

Data simulation and analysis

Figures 5 shows the analysis results for $k_{Pi\rightarrow\gamma\text{-}ATP}$ using the m_{Pi} and $m_{\gamma ATP}$ datasets generated at given $k_{Pi\rightarrow\gamma\text{-}ATP}$ and $T_{1,Pi}$ values and mixed with random noises. For a large number of executions (N = 1000), the mean values obtained for $k_{Pi\rightarrow\gamma\text{-}ATP}$ by these four different data analysis approaches are very similar to the input value ($k_{Pi\rightarrow\gamma\text{-}ATP} = 0.07$ sec^{-1}), but each approach shows a different dispersion pattern, as indicated by the data histograms (Figure 5). A significant large variance in $k_{Pi\rightarrow\gamma\text{-}ATP}$ is noticed in the histogram by Eq [3b] approach, as compared to other three methods defined by Eqs [3], [3a] and [11], suggesting it may be a less favorable approach. Among the three remaining approaches with smaller variances, Eqs [3] and [11] yielded slightly better outcomes in $k_{Pi\rightarrow\gamma\text{-}ATP}$ in terms of mean and standard deviation (Figure 5). Similar features also appear in the histograms for $T_{1,Pi}$ analysis results (Supplementary Figure S2).

For the three different time-saving acquisition strategies examined by simulation, it is found that a 100% increase in noise level (simulation S1), equivalent to a 4-fold decrease in NA and scan time, led to a 100% increase in variance in $k_{Pi\rightarrow\gamma\text{-}ATP}$ (Figures 5), as evaluated by Eqs [3], [3a] and [11]. A comparison between the two scenarios with 50% reduced data points (S2 and S3) indicates that the strategy with larger sampling intervals (S3) appears to be a better choice for $k_{Pi\rightarrow\gamma\text{-}ATP}$ determination. The $T_{1,Pi}$ analysis on the same simulation datasets showed the similar findings (Supplementary Figure S2).

For those three linear equations (Eqs [3], [3a] and [3b]), an obvious feature is the absence of $T_{1app,\gamma\text{-}ATP}$, in contrast to Eq [11] in which $T_{1app,\gamma\text{-}ATP}$ is an unknown that has to be solved in order to get $k_{Pi\rightarrow\gamma\text{-}ATP}$. Simulations were performed to test whether a change in $T_{1app,\gamma ATP}$ would affect $k_{Pi\rightarrow\gamma\text{-}ATP}$ determination. For the two linear approaches defined by Eqs. [3 and 3a], simulation results (Figure 6) indicate that there was no significant difference in mean $k_{Pi\rightarrow\gamma\text{-}ATP}$ value when $T_{1app,\gamma ATP}$ was varied from 1 to 6 sec; the obtained

$k_{Pi\rightarrow\gamma\text{-}ATP}$ values were comparable to that by the matrix approach defined by Eq [11] and consistent with the input value. However, the difference in $k_{Pi\rightarrow\gamma\text{-}ATP}$ between the linear approach by Eq [3b] and other approaches is noticeably large (Figure 6). Especially, the variance in $k_{Pi\rightarrow\gamma\text{-}ATP}$ by Eq [3b] was increased dramatically when $T_{1app,\gamma ATP}$ was decreased from 4 to 1 sec, suggesting that Eq [3b] approach may not be reliably applicable for $k_{Pi\rightarrow\gamma\text{-}ATP}$ determination when γ-ATP relaxation is fast. At $T_{1app,\gamma ATP}$ = 1 sec, which is equivalent to narrow band selective inversion, the matrix approach defined by Eq [11] yielded the best performance (Figure 6), with a variance ~2 – 3 fold smaller than those by Eqs [3] and [3a]. Similar performance was also found in $T_{1,Pi}$ analysis (Supplementary Figure S3) in which a large variance in $T_{1,Pi}$ was given by Eq [3b] approach, as compared to other approaches.

DISCUSSION

Although the ability to probe exchange kinetics between metabolites using IT techniques has long been recognized, its use has behind alternative ST techniques for measurement of ATP synthesis rates (commentary (17) and the references therein). The added chemical shift dispersion and sensitivity of high field research scanners provide the motivation to reexamine the possible benefits of measuring such exchanges in vivo using IT methods (6). The preference of ST over IT may also have much to do with the ease of data analysis in ST, which permits the evaluation of $k_{Pi\rightarrow ATP}$ by a simple expression, rather than a non-intuitive way as in IT, numerically solving two or more simultaneous equations with multiple unknown parameters. Certain strategies toward simplifying IT data analysis were suggested in early kinetic studies. For example, early studies (4,5) showed that the rate constant for a two-spin system can be obtained from the initial slope of the curve $M_z(t) \sim t$ by a formula equivalent to Eq [8]. derived directly from the basic Bloch-McConnell equation. In 1990 Kuchel (1) also proposed a simple formula, equivalent to Eq [7], to calculate the rate constant based on the inverted and non-inverted magnetizations at the time point with $\dot{m} = 0$ (for non-inverted spin).

In the current study, we suggest a method to directly utilize $\dot{m}_{Pi}$, as defined by the original Bloch-McConnell equation for analysis of $k_{Pi\rightarrow\gamma\text{-}ATP}$. The $\dot{m}_{Pi}$ data can be easily derived from the experimental m_{Pi} data (Eqs [5] and [6], and Figures 3a and 3b). Unlike m_{Pi}, which has a complex relationship with k (5), $\dot{m}_{Pi}$ is linearly correlated to k (Eq [3]), with a simple proportional coefficient ($m_{Pi} - m_{\gamma ATP}$). As illustrated in Figure 3b, the trend in $\dot{m}_{Pi} \sim t$ is governed by two counteractive terms, the exchange term $k_{Pi\rightarrow\gamma ATP}(m_{Pi} - m_{\gamma ATP})$, which measures the magnitude of the net ME flux, and the relaxation term $(1 - m_{Pi})/T_{1,Pi}$, which measure the magnitude of T_1 relaxation effect at Pi.

Once $\dot{m}_{Pi}$ is derived, one can easily determine $k_{Pi\rightarrow\gamma ATP}$ and $T_{1,Pi}$ by Eq [3, 3a or 3b], each having certain advantages and limitations. Eqs [3a and 3b] both are visually intuitive, with $k_{Pi\rightarrow\gamma ATP}$ and $1/T_{1,Pi}$ shown as the slope and intercept (or vice versa) of a visible line while Eq [3] provides a direct quantitative separation of relaxation and exchange terms (Figure 4b), from which one can easily understand how these two terms evolve with delay time and contribute to the observed ME effect.

Despite the difference in mathematical expression, for resting human calf muscle, the data analysis using Eqs [3, 3a and 3b] yielded comparable $k_{Pi\rightarrow\gamma ATP}$ results, as that by the numerical matrix approach defined by Eq [11] (Table 1). These results are also in agreement with the corresponding $k_{Pi\rightarrow\gamma ATP}$ value (0.050 s^{-1}) by an integrated numerical analysis method on data acquired using EKIT sequence (6). They are also consistent with the literature reported $k_{Pi\rightarrow\gamma ATP}$ values ranging from 0.04 to 0.12 s^{-1} using ST approach (review (9) and the references therein). The $T_{1,Pi}$ relaxation times obtained by these linear approaches are also in reasonably agreement with the literature values (6,37) at 7T.

It should be noted that, although the IT technique is not able to decouple Pi from the rest of the ^{31}P exchange network in vivo as ST does through prolonged irradiation at γ-ATP, the IT data analysis method presented here requires no detailed knowledge about the various exchange reaction that the inverted γ-ATP is involved for evaluation of $k_{Pi\rightarrow\gamma ATP}$. This means that, selection of IT or ST techniques depends on practical considerations such as available sequences in the MRI scanner and the required experimental time. Since IT technique does not require additional mirror irradiation to control the “spillover” effect, it is an advantage over progressive ST on this respect.

A careful analysis of the simulated datasets indicates that it is possible to get reliable rate constant $k_{Pi\rightarrow\gamma ATP}$ by using fewer data points or fewer acquisition averages to save scan time. One most attractive strategy is to acquire data at relatively large intervals to cover a wide range of delay times (simulation S3). It is possible that one can complete the data acquisition with ~10 minutes and still able to obtain reliable $k_{Pi\rightarrow\gamma ATP}$ values. While all linear approaches presented here are mathematically simpler than the numerical matrix approach, the linear data analysis approach defined by Eq [3a] offers less variance values and larger suitability range (Figures 5–6).

In summary, we demonstrated that, using simple linear fitting procedure, IT data acquired by band inversion technique can be used to derive the $k_{Pi\rightarrow\gamma ATP}$ parameter for evaluation of the physiologically important Pi → ATP flux. Band inversion transfer is one alternative to ST for the measurement of ATP synthesis in vivo.

Supplementary Material

Refer to Web version on PubMed Central for supplementary material.

ACKNOWLEDGEMENTS

The authors are grateful for the technical support from Drs. Baolian Yang and Ivan Dimitrov (Philips Medical Systems), Salvador Pena for operational assistance. Jeannie Davis and Janet Jerrow recruited and managed the human subjects. This project was supported by the National Center for Research Resources and the National Institute of Biomedical Imaging and Bioengineering of the National Institutes of Health through P41EB015908, DK081186, R37HL034557, P01DK058398 and R01AR050597, Department of Defense Grant W81XWH-06-2-0046.

Abbreviation used

IT	inversion transfer

ST	saturation transfer
NOE	nuclear Overhauser effect
ME	magnetization exchange
MT	magnetization transfer
SAR	specific absorption ratio
EKIT	exchange kinetics by inversion transfer
EBIT	exchange kinetics by band inversion transfer
Eq	Equation
Pi	inorganic phosphate
ATP	adenosine triphosphate
ADP	adenosine diphosphate
PCr	phosphocreatine
PDE	phosphodiesters
CK	creatine kinase
AK	adenylate kinase
PFK	phosphofructokinase
GAPDH	glyceraldehydes-3-phosphate dehydrogenase

REFERENCES

1. Kuchel PW. Spin-exchange NMR spectroscopy in studies of the kinetics of enzymes and membrane transport. NMR Biomed. 1990; 3(3):102–119. [PubMed: 2201390]
2. Noggle, JH.; Schirmer, RE. The nuclear overhauser effect - chemical applications. New York and London: Acedemic press; 1971.
3. Meyer RA, Kuchmerick MJ, Brown TR. Application of 31P-NMR spectroscopy to the study of striated muscle metabolism. Am J Physiol. 1982; 242(1):C1–C11. [PubMed: 7058872]
4. Alger JR, Prestegard JH. Investigation of peptide bond isomerization by magnetization transfer NMR. J Magn Reson. 1977; 27(1):137–141.
5. Malloy CR, Sherry AD, Nunnally RL. Carbon 13 NMR measurement of flux through alanine animotransferase by inversion and saturation transfer methods. J Mag Res. 1985; 64:243–254.
6. Ren J, Yang B, Sherry AD, Malloy CR. Exchange kinetics by inversion transfer: Integrated analysis of the phosphorous metabolite kinetics exchanges in resting human skeletal muscle at 7T. Magn Reson Med. 2014
7. Brown TR, Ugurbil K, Shulman RG. 31P nuclear magnetic resonance measurements of ATPase kinetics in aerobic Escherichia coli cells. Proc Natl Acad Sci USA. 1977; 74(12):5551–5553. [PubMed: 146199]
8. Kingsley-Hickman P, Sako EY, Andreone PA, St Cyr JA, Michurski S, Foker JE, From AH, Petein M, Ugurbil K. 31P NMR measurement of ATP synthesis rate in perfused intact rat hearts. FEBS Lett. 1986; 198(1):159–163. [PubMed: 2869973]

9. Kemp GJ, Brindle KM. What do magnetic resonance-based measurements of Pi→ATP flux tell us about skeletal muscle metabolism? Diabetes. 2012; 61(8):1927–1934. [PubMed: 22826313]
10. Befroy DE, Rothman DL, Petersen KF, Shulman GI. 31P-magnetization transfer magnetic resonance spectroscopy measurements of in vivo metabolism. Diabetes. 2012; 61(11):2669–2678. [PubMed: 23093656]
11. Petersen KF, Befroy D, Dufour S, Dziura J, Ariyan C, et al. Mitochondrial dysfunction in the elderly: Possible role in insulin resistance. Science. 2003; 300:1140–1142. [PubMed: 12750520]
12. Petersen KF, Dufour S, Shulman GI. Decreased insulin-stimulated ATP synthesis and phosphate transport in muscle of insulin-resistant offspring of type 2 diabetic parents. PLoS Med. 2005; 2(9):e233. [PubMed: 16089501]
13. Lowell BB, Shulman GI. Mitochondrial dysfunction and type 2 diabetes. Science. 2005; 307:384–387. [PubMed: 15662004]
14. Szendroedi J, Schmid AI, Chmelik M, Toth C, Brehm A, et al. Muscle Mitochondrial ATP Synthesis and Glucose Transport/Phosphorylation in Type 2 Diabetes. PLoS Med. 2007; 4(5):e154. [PubMed: 17472434]
15. Petersen KF, Dufour S, Befroy D, Garcia R, Shulman GI. Impaired mitochondrial activity in the insulin-resistant offspring of patients with type 2 diabetes. N Engl J Med. 2004; 350:664–671. [PubMed: 14960743]
16. Lebon V, Dufour S, Petersen KF, Ren J, Jucker BM, et al. Effect of triiodothyronine on mitochondrial energy coupling in human skeletal muscle. J Clin Invest. 2001; 108:733–737. [PubMed: 11544279]
17. Jucker BM, Dufour S, Ren J, Cao X, Previs SF, Underhill B, Cadman KS, Shulman GI. Assessment of mitochondrial energy coupling in vivo by 13C/31P NMR. Proc Natl Acad Sci U S A. 2000; 97(12):6880–6884. Erratum in: Proc Natl Acad Sci U S A 2001; 98(6):3624. [PubMed: 10823916]
18. Koretsky AP, Basus VJ, James TL, Klein MP, Weiner MW. Detection of exchange reactions involving small metabolite pools using NMR magnetization transfer techniques: relevance to subcellular compartmentation of creatine kinase. Magn Reson Med. 1985; 2(6):586–594. [PubMed: 3880100]
19. Balaban RS, Koretsky AP. Interpretation of ^{31}P NMR saturation transfer experiments: what you can't see might confuse you. Focus on "Standard magnetic resonance-based measurements of the Pi→ATP rate do not index the rate of oxidative phosphorylation in cardiac and skeletal muscles". Am J Physiol Cell Physiol. 2011; 301(1):C12–C15. [PubMed: 21490314]
20. Nabuurs CI, Hilbers CW, Wieringa B, Heerschap A. Letter to the editor: "Interpretation of 31P NMR saturation transfer experiments: do not forget the spin relaxation properties". Am J Physiol Cell Physiol. 2012; 302(10):C1566–C1567. [PubMed: 22492653]
21. Kingsley PB, Monahan WG. Corrections for off-resonance effects and incomplete saturation in conventional (two-site) saturation-transfer kinetic measurements. Magn Reson Med. 2000; 43(6): 810–819. [PubMed: 10861875]
22. Baguet E, Roby C. Off-Resonance Irradiation Effect in Steady-State NMR Saturation Transfer. J Magn Reson. 1997; 128(2):149–160. [PubMed: 9356270]
23. Valkovič L, Bogner W, Gajdošík M, Považan M, Kukurová IJ, Krššák M, Gruber S, Frollo I, Trattnig S, Chmelík M. One-dimensional image-selected in vivo spectroscopy localized phosphorus saturation transfer at 7T. Magn Reson Med. 2014 In press.
24. Degani H, Laughlin M, Campbell S, Shulman RG. Kinetics of creatine kinase in heart: a 31P NMR saturation- and inversion-transfer study. Biochemistry. 1985; 24(20):5510–5516. [PubMed: 4074712]
25. Brown TR, Ogawa S. 31P nuclear magnetic resonance kinetic measurements on Adenylate kinase. Proc Natl Acad Sci. 1972; 74:3627–3631. [PubMed: 198793]
26. Brindle KM. NMR methods for measuring enzyme kinetics in vivo. Progress in NMR Spectroscopy. 1988; 20:257–293.
27. Morris GA, Freeman R. Selective excitation in Fourier transform nuclear magnetic resonance. J Magn Reson. 1978; 29:433–462.

28. Schmid AI, Schrauwen-Hinderling VB, Andreas M, Wolzt M, Moser E, Roden M. Comparison of measuring energy metabolism by different (31) P-magnetic resonance spectroscopy techniques in resting, ischemic, and exercising muscle. Magn Reson Med. 2012; 67(4):898–905. [PubMed: 21842500]
29. Valkovič L, Chmelík M, Just Kukurova I, Krššák M, Gruber S, Frollo I, Trattnig S, Bogner W. Time-resolved phosphorous magnetization transfer of the human calf muscle at 3 T and 7 T: a feasibility study. Eur J Radiol. 2013; 82(5):745–751. [PubMed: 22154589]
30. Brindle KM, Blackledge MJ, Challiss RA, Radda GK. 31P NMR magnetization-transfer measurements of ATP turnover during steady-state isometric muscle contraction in the rat hind limb in vivo. Biochemistry. 1989; 28(11):4887–4893. [PubMed: 2765517]
31. Shoubridge EA, Briggs RW, Radda GK. 31P NMR saturation transfer measurements of the steady state rates of creatine kinase and ATP synthetase in the rat brain. FEBS Lett. 1982; 140(2):289–292. [PubMed: 6282642]
32. Lei H, Ugurbil K, Chen W. Measurement of unidirectional Pi to ATP flux in human visual cortex at 7 T by using in vivo 31P magnetic resonance spectroscopy. Proc Natl Acad Sci U S A. 2003; 100(24):14409–14414. [PubMed: 14612566]
33. Du F, Zhu XH, Qiao H, Zhang X, Chen W. Efficient in vivo 31P magnetization transfer approach for noninvasively determining multiple kinetic parameters and metabolic fluxes of ATP metabolism in the human brain. Magn Reson Med. 2007; 57(1):103–114. [PubMed: 17191226]
34. Nabuurs C, Huijbregts B, Wieringa B, Hilbers CW, Heerschap A. 31P saturation transfer spectroscopy predicts differential intracellular macromolecular association of ATP and ADP in skeletal muscle. J Biol Chem. 2010; 285(51):39588–39596. [PubMed: 20884612]
35. Ren J, Sherry AD, Malloy CR. Amplification of the effects of magnetization exchange by band inversion for measuring adenosine triphosphate synthesis rates in human skeletal muscle. Magn Reson Med. 2014
36. Xiong Q, Du F, Zhu X, Zhang P, Suntharalingam P, Ippolito J, Kamdar FD, Chen W, Zhang J. ATP production rate via creatine kinase or ATP synthase in vivo: a novel superfast magnetization saturation transfer method. Circ Res. 2011; 108(6):653–663. [PubMed: 21293002]
37. Bogner W, Chmelik M, Schmid AI, Moser E, Trattnig S, Gruber S. Assessment of (31)P relaxation times in the human calf muscle: a comparison between 3 T and 7 T in vivo. Magn Reson Med. 2009; 62(3):574–582. [PubMed: 19526487]

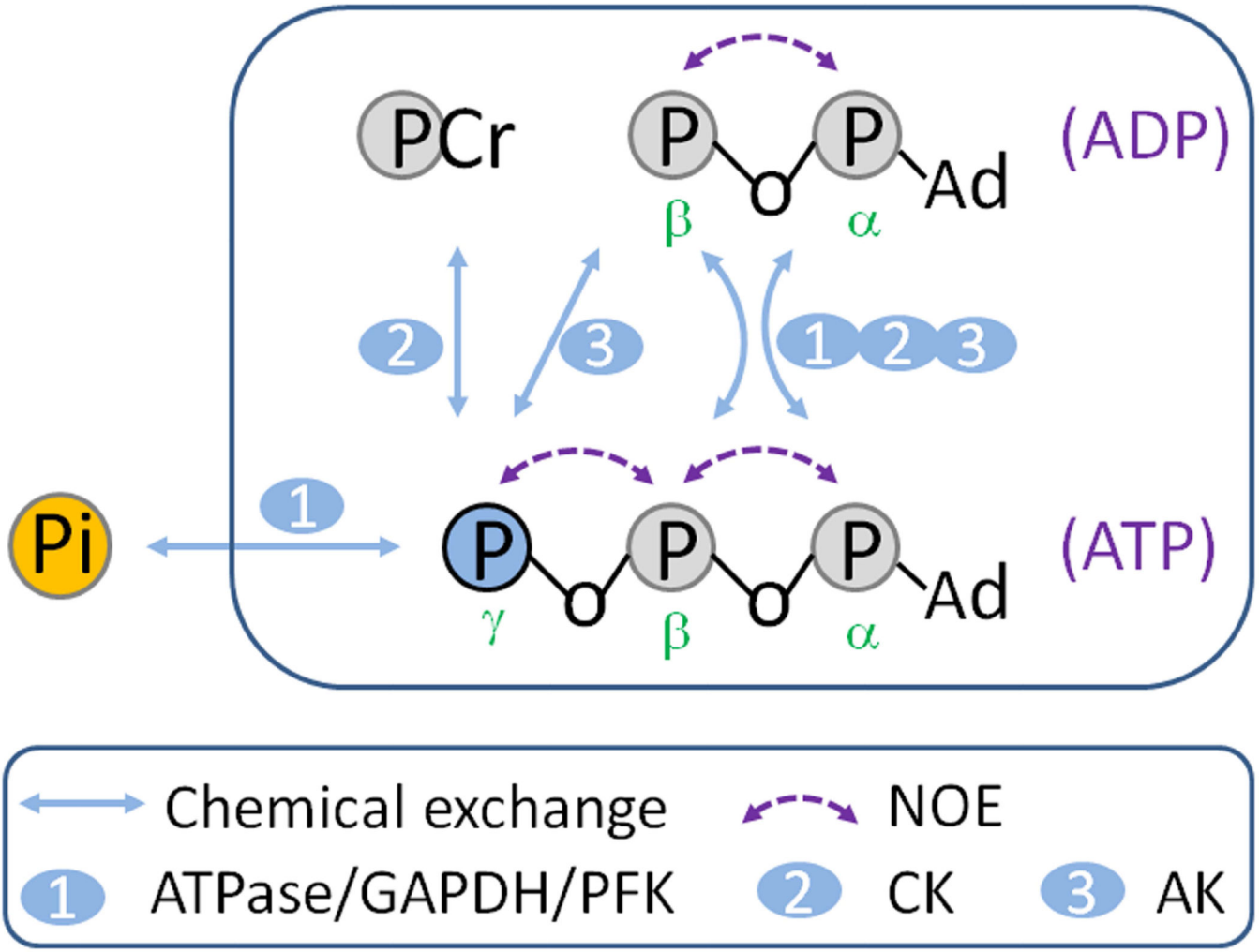

FIG. 1.

Possible ^{31}P magnetization exchange pathways in skeletal muscle. Abbreviations: CK, creatine kinase; AK adenylate kinase; PFK, phosphofructokinase; GAPDH, glyceraldehyde 3-phosphate dehydrogenase; NOE, nuclear Overhauser effect.

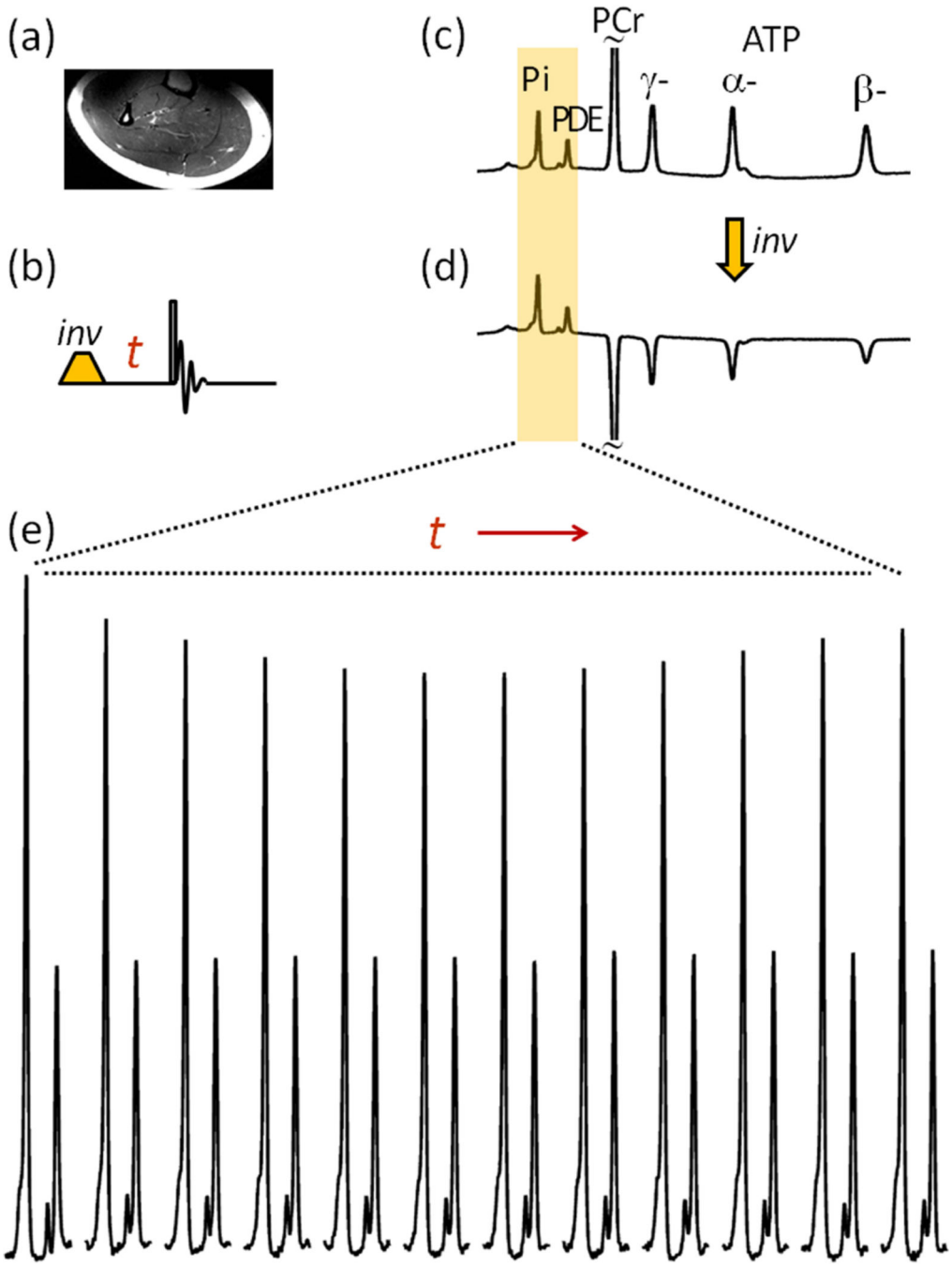

FIG. 2.

Image and ^{31}P NMR of Human Calf Muscle. (a) T2w MR image. (b) Sequence of the band-selective inversion pulse used in the experiment. (c) and (d) ^{31}P NMR spectra acquired from resting muscle before (c) and after (d) applying the band inversion sequence. (e) Evolution of the Pi signal with the inversion delay time *t*. The spectral data represents averages for n = 15 subjects.

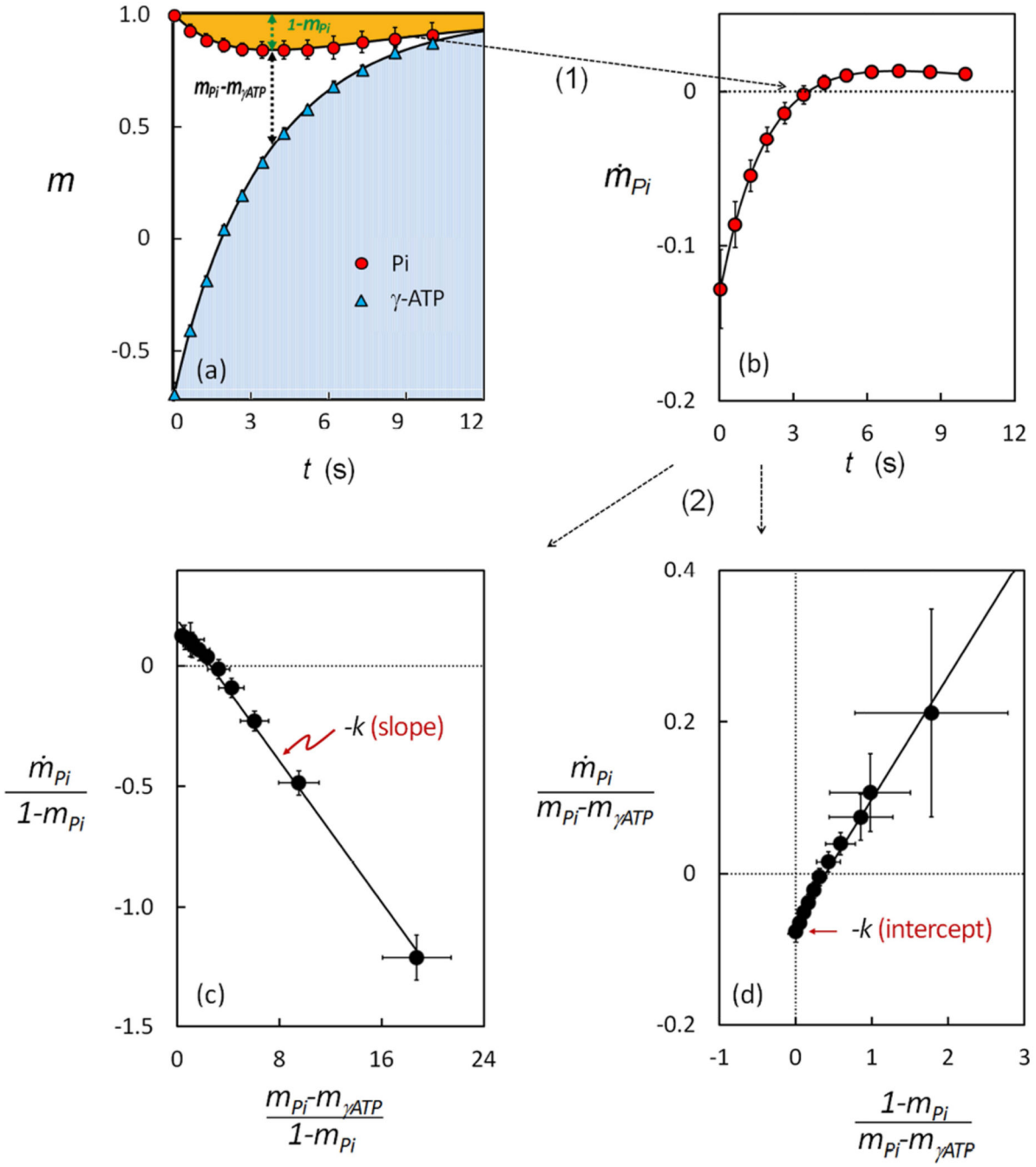

FIG. 3.

Alternative Analyses of Band Inversion-Transfer Data Sets (n = 15 subjects). (a) The m-plot, showing dependence of Pi and γ-ATP magnetization (m_{Pi} and $m_{\gamma ATP}$) on inversion delay time t. (b) The $\dot{m}$–plot, showing the rate of change of Pi signal with inversion delay time t. (c) The linear relationship between $\frac{\dot{m}_{Pi}}{1-m_{Pi}}$ and $\frac{m_{Pi}-m_{\gamma ATP}}{1-m_{Pi}}$, with a slope defined by -$k_{Pi\rightarrow\gamma ATP}$ and an intercept defined by $1/T_{1,Pi}$. (d) The linear relationship between

$\frac{\dot{m}_{P_i}}{m_{P_i} - m_{\gamma ATP}}$ and $\frac{1 - m_{Pi}}{m_{Pi} - m_{\gamma ATP}}$, with a slope defined by $1/T_{1,Pi}$ and an intercept defined by - $k_{Pi \rightarrow \gamma ATP}$.

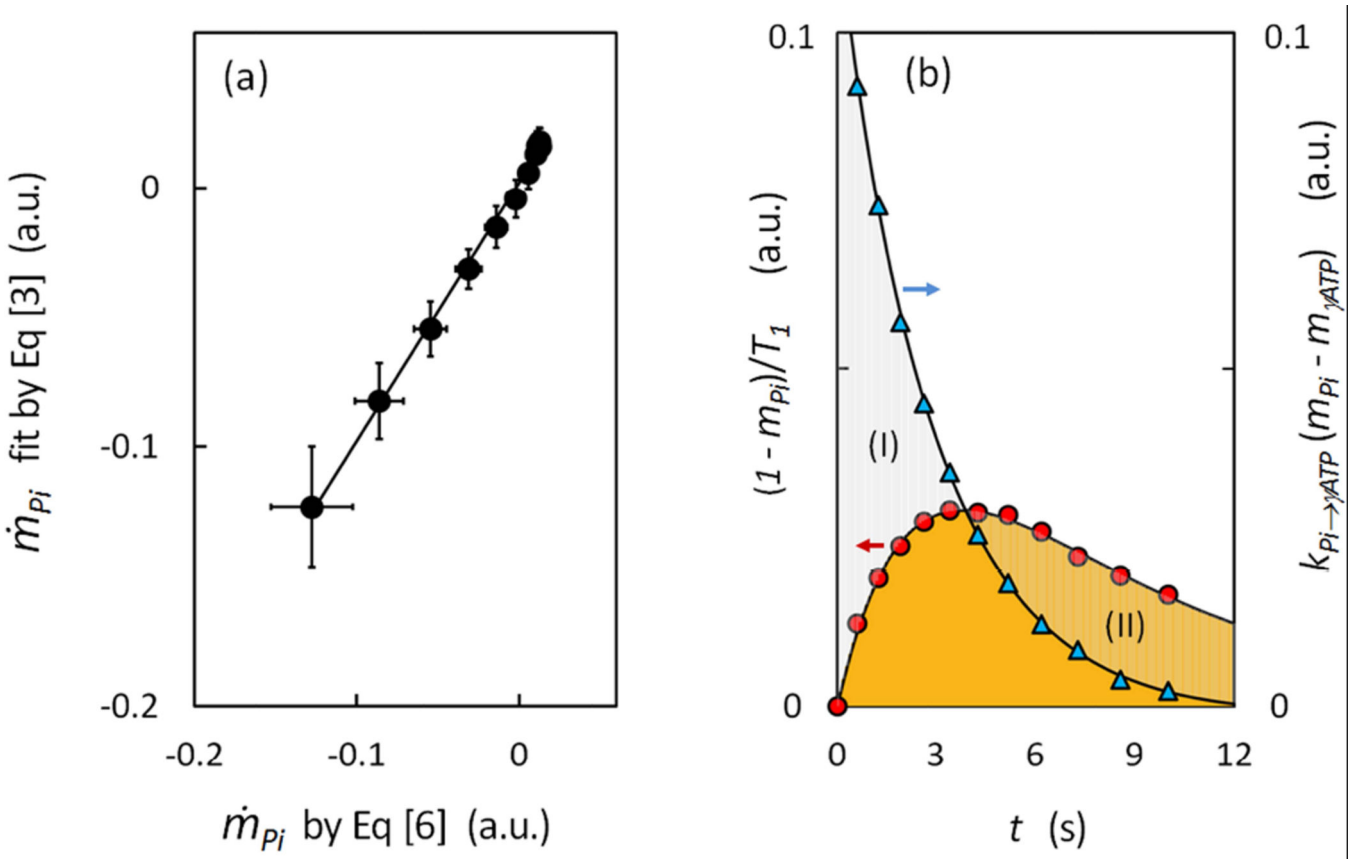

FIG. 4.

Analysis of Relaxation and Exchange Components in Rate of Change of Pi Signal. (a) Linear correlation of $\dot{m}_{Pi}$ data derived by Eq [6] and those by fitting to Eq [3] (n = 15 subjects). The resultant fitting parameters $k_{Pi\rightarrow\gamma ATP}$ and $T_{1,Pi}$ are presented in (b) with a multiplication factor ($m_{Pi} - m_{\gamma ATP}$) and ($1 - m_{Pi}$) to separate the relaxation term from the exchange term in $\dot{m}_{Pi}$ as defined by Eq [3]. The region marked by (I) indicates the dominance of the exchange term over the relaxation term, and the opposite for the region marked by (II).

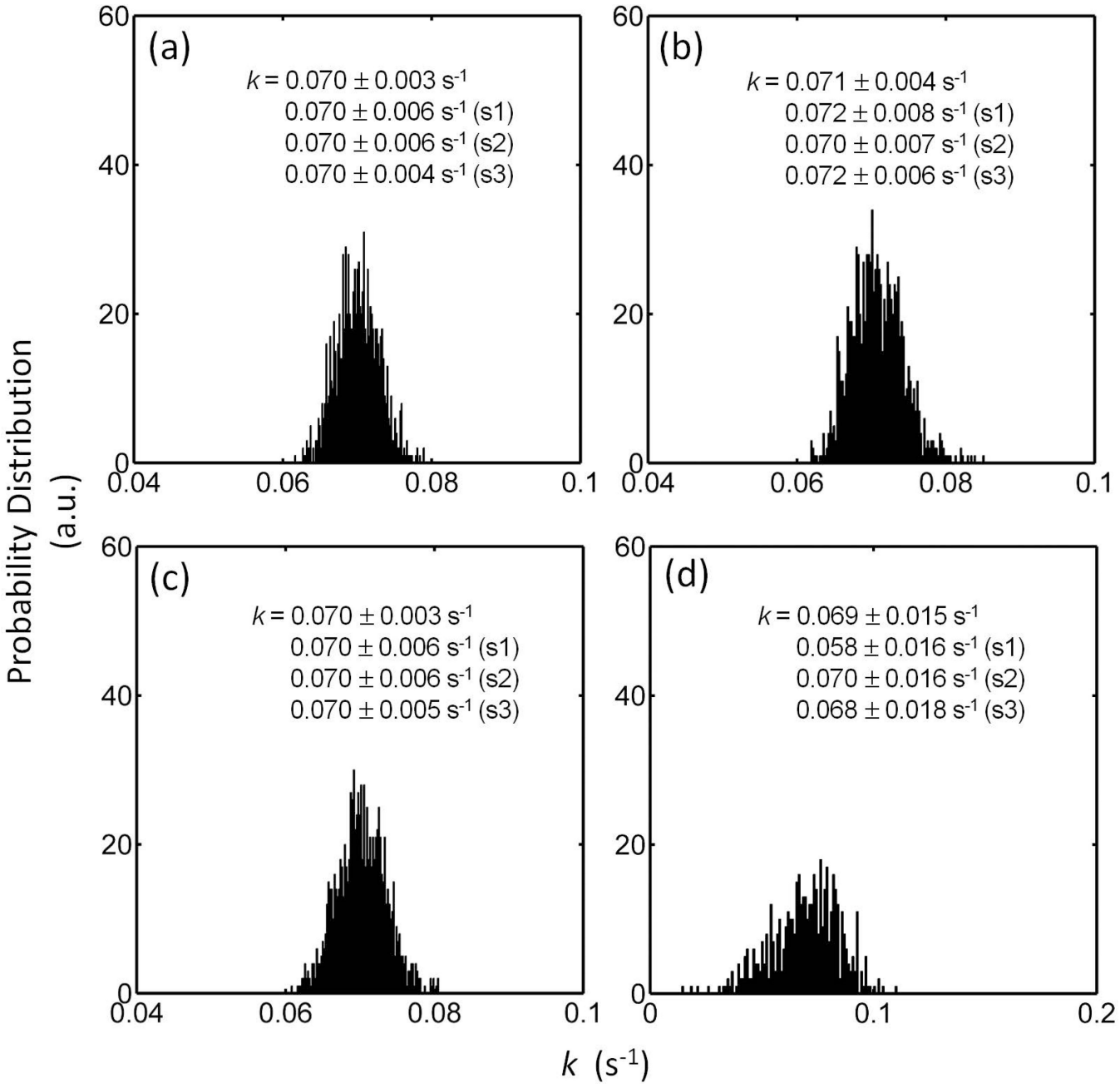

FIG. 5.

Effects of Noise on Evaluation of $k_{Pi\rightarrow\gamma ATP}$. The histograms represent the results of 1000 datasets in simulation of a scan with 12 data points at noise level ± 1%, using analysis approaches defined by Eqs [11] (a), [3] (b), [3a] (c) and [3b] (d). The derived $k_{Pi\rightarrow\gamma ATP}$ results are compared with those obtained for simulation at a higher noise level of ± 2% (S1), simulation of a scan collecting only the first 6 data points (S2), and simulation of a scan with 6 data points at large intervals in a wide range of delay times (S3).

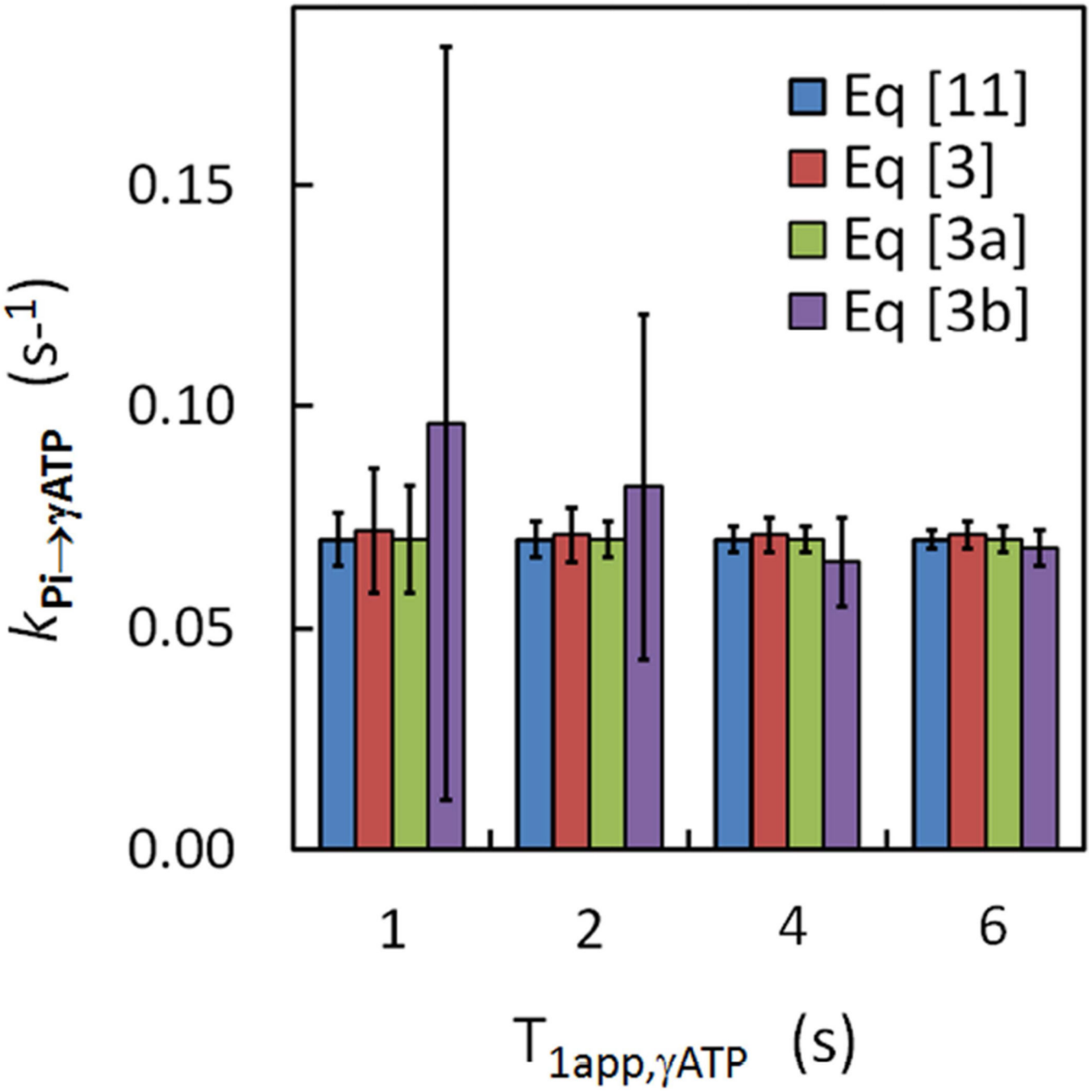

FIG. 6.

Effects of $T_{1app,\gamma ATP}$ on analysis of $k_{Pi\rightarrow\gamma ATP}$. Comparison of different fitting approaches on analysis of simulation data at different apparent T_1 values for γ-ATP.

Table 1

Unidirectional rate constant for the ATP synthesis reaction Pi → γ-ATP in resting human skeletal muscle (n = 15)

$k_{Pi\rightarrow\gamma\text{-}ATP}$ (s^{-1})	Fitting equation
0.067 ± 0.012	Eq. [11]
0.068 ± 0.014	Eq. [3]
0.069 ± 0.017	Eq. [3a]
0.061 ± 0.019	Eq. [3b]